



WWTP effluent treatment with ultrafiltration with different mixed matrix nanocomposite membranes. Comparison of performance and fouling behavior

Gabriela Kamińska

Institute of Water and Wastewater Engineering, Gliwice, Poland

Corresponding author's e-mail: gabriela.kaminska@polsl.pl

Keywords: ultrafiltration, fouling, micropollutants, nanocomposite membranes, WWTP effluent

Abstract: Polymer mixed-matrix nanocomposite membranes were prepared by a wet-phase inversion method and used in ultrafiltration processes to treat wastewater treatment plant effluent spiked with organic micropollutants. The effects of halloysite (Hal), TiO₂, and functionalized single-walled carbon nanotube (SWCNT-COOH) nanofillers on the treatment efficiency, permeability loss, and fouling behavior of polyethersulfone (PES) membranes were investigated and compared with those of a pristine PES membrane. The nanocomposite membranes exhibited lower porosity and stronger negative surface charge because of the added hydrophilic nanofillers. The PES-Hal membrane achieved the optimal balance of permeability and micropollutant removal owing to enhanced pollutant adsorption on the membrane surface and the creation of an easily removable cake layer (i.e., reversible fouling). The PES-SWCNT-COOH membrane demonstrated the highest treatment efficiency, but also the high permeability loss. In contrast, PES-TiO₂ exhibited excellent antifouling properties, but poorer treatment capabilities.

Introduction

Water pollution is currently one of the greatest concerns around the world. The quality of surface water is directly linked to wastewater treatment. Recently, many countries have introduced new standards in wastewater treatment, which have led to improvements in the quality of effluent, and consequently, of surface water. They aim to remove all nutrients, suspended solids, dissolved solids, toxic pathogens, and emerging micropollutants from the WWTP (wastewater treatment plant) effluent.

Ultrafiltration has been demonstrated to be a very effective and economical method for removing pollutants, while providing flexibility by implementing various membrane materials (e.g., ceramics, polymers) with distinct functional properties (e.g., molecular weight cut off, porosity, hydrophilicity/hydrophobicity, surface charge, water permeability, thickness, mechanical stability, thermal resistance) [Haas et al. 2019]. However, membrane fouling is a significant difficulty affecting the permeability of ultrafiltration membranes [Bu et al. 2019].

One approach to mitigate membrane fouling is to employ membranes with good antifouling properties. Thus, novel nanocomposite membranes are garnering attention [Bassouini et al. 2019]; they represent a promising type of modified polymer membrane for water/wastewater treatment, which exhibit three key advantages, i.e., improved permeation, enhanced rejection, and reduced fouling [Esfahani et al. 2019]. The most popular

nanofillers for these novel nanocomposite membranes include carbon nanotubes, graphene, nanoclays (e.g., montmorillonite, halloysite, bentonite, zeolite), nano metal oxides (e.g., TiO₂, ZnO), and nanocrystals (e.g., nanocrystalline cellulose) [Buruga et al. 2019, Bodzek et al. 2021]. Modifying the membranes based on the nanofiller affects their water permeation, contaminant rejection, and antifouling capabilities by altering one or more physicochemical properties, such as the porosity, pore size, hydrophilicity/hydrophobicity, membrane surface charge, and/or roughness [Nasir et al. 2019].

The addition of carbon nanotubes, graphene, or nanoclays may enhance the rejection of contaminants due to solute adsorption on the membrane surface [Kamińska et al. 2016]. Dudziak et al. [2017] improved the properties of polyethersulfone (PES) ultrafiltration membranes via loading with single-walled carbon nanotubes. The modified membrane achieved an increased permeate flux and rejection of 17 β -estradiol and bisphenol A at a maximum level of 70%; for comparison, rejection of these compounds by a virgin PES membrane reached only 30%. Shakak et al. [2019] proposed that nanocomposite ultrafiltration polysulfone/polyvinylpyrrolidone (PSF/PVP) membranes modified with SiO₂ nanoparticles exhibited superb antifouling properties and amoxicillin removal efficiencies. Specifically, amoxicillin retention increased from 66.5% to 89.9% when the loading of SiO₂ nanoparticles increased from 0 to 4 wt.%. They correlated the enhanced retention with the Donnan electrostatic

force mechanism and repulsive forces between the anionic amoxicillin and the negatively-charged membrane surface. Small, hydrophilic amoxicillin molecules cannot be retained via adsorption or size exclusion mechanisms. Similarly, the addition of montmorillonite to a PES membrane enhanced its retention of nitrophenols through adsorption and electrostatic repulsion effects between the charged compound and similar charges on the membrane surface [Ghaemi et al. 2011].

Membranes containing nanofillers with oxygen function groups have a lower fouling tendency [Kamińska et al. 2015]. For example, the low degree of fouling of a PES membrane modified with boehmite was attributed to the lower roughness and a higher hydrophilicity of the membrane surface [Vatanpour et al. 2012]. Mozia et al. [2019] reported that modification with halloysite positively influenced the hydrophilicity, water permeability, and antifouling properties of PES membranes because of the –OH groups on halloysite. TiO₂ is another nanofiller that positively influences the antifouling properties of polymer membranes [Zhang et al. 2014]. Nanocomposite membranes have also been employed to treat industrial wastewater to mitigate fouling and increase the treatment efficiency [Shaban et al. 2019].

A wide variety of nanofillers have been used to develop numerous types of nanocomposite membranes with low fouling tendencies or enhanced treatment efficiencies. Nevertheless, the available literature data does not clarify which nanofillers are the most beneficial for simultaneous pollutant removal and fouling mitigation during the treatment of WWTP effluent. To date, most studies have been focused on removing one group of pollutants with nanocomposite membranes; however, most environmental samples contain both organic and inorganic contaminants [Kamińska 2022]. Therefore, a novelty of this study is to compare the fouling tendencies and separation capabilities of three nanocomposite membranes in the treatment of WWTP effluent spiked with organic micropollutants having various chemical properties. The compounds selected for this study include caffeine (CAF), benzotriazole (BZT), carbamazepine (CBZ), and bisphenol A (BPA), which commonly exist in aquatic environments and represent the main types of hazardous environmental micropollutants, e.g., psychostimulants, corrosion inhibitors, pharmaceuticals, and xenoestrogens, respectively [Rogowska et al 2020].

From various types of nanoparticles, halloysite nanoclay (Hal), single-walled carbon nanotubes functionalized with carboxyl groups (SWCNT-COOH), and TiO₂ nanoparticles (TiO₂) were used as the nanofillers for membrane modifications due to their high specific surface area and adsorptive properties

(Hal, SWCNT-COOH) and hydrophilicity (Hal, SWCNT-COOH, TiO₂). The high specific surface area of nanofillers can improve retention characteristics of membranes, while hydrophilicity can improve their antifouling properties.

To the best of my knowledge, this is a first time when effect of different nanofillers on performance of nanocomposite membranes is reported. Most current papers describe an effect of different concentrations of one type of nanofiller.

Methodology

Materials

Polyethersulfone (Ultrason S) was provided by BASF (Ludwigshafen, Germany); Hal was obtained from Sigma Aldrich (Poznań, Poland); SWCNT-COOH were obtained from Chengdu Organic Chemistry Co. Ltd. (Chengdu, China); TiO₂ was provided by Hongwu International Group Ltd. (Guangzhou, China). The properties of nanoparticles are presented in Table 1. Ultrapure water was obtained directly from a Rephile water purification system (Rephile Bioscience Ltd., Shanghai, China). Acetonitrile (ACN), methanol (MeOH), and dimethylformamide (DMF) were purchased from Avantor Performance Materials (Gliwice, Poland). Caffeine, benzotriazole, carbamazepine, and bisphenol A (purity = 99% for all) were purchased from Sigma Aldrich (Poznań, Poland).

Membrane preparation

Three polymer matrix nanocomposite membranes (PES-Hal, PES-SWCNT-COOH, and PES-TiO₂) were prepared using a phase-inversion method. The casting solution consisted of 14.9 wt.% PES, 0.1 wt.% fillers, and 85 wt.% DMF. This composition was recognized as the most favorable in previous study to obtain ultrafiltration membranes [Kamińska 2022]. Loading of 0.1%wt. of nanofillers was also recommended in many other reports to obtain membranes with the best performance [Ghaemi 2011, Mozia 2019, Vatanpour 2012]. Membranes were prepared as follows: first, the nanofiller was added to the DMF, and the resulting suspension was subjected to ultrasonication; then, an appropriate amount of PES was added, and casting solution was shaken for 20 h to obtain a homogeneous solution; additionally, a virgin PES membrane containing 15:85 (w/w) of PES:DMF was prepared in an analogous manner. The membranes were cast on glass plates using an automatic film applicator (Elcometer 4340, Elcometer Ltd., Manchester, UK) with a knife gap of 220 μm and immediately immersed in deionized water at ~20°C. The precipitated membranes were stored in deionized water at 7°C for 24 h to maintain their stabilization.

Table 1. Properties of nanofillers

Property	Hal	SWCNT-COOH	TiO ₂
Outer diameter (nm) ¹	50–100	1–2	10–15
Length (μm) ¹	0.5	5–30	>1
Purity (wt%) ¹	–	90	–
COOH content (%) ¹	–	2.7	–
SSA (m ² /g) ²	50.4	425.9	300

¹ Data provided by manufacturer, ² – own measurements.

Membrane characterization

The dynamic viscosities of the membrane casting solutions were measured using a rolling ball viscometer (Lovis 2000 M/ME, Anton Paar, Graz, Austria) with a steel ball and a Lovis capillary (diameter = 2.5 mm). The cross-section morphologies of the membranes were investigated via scanning electron microscopy (SEM; Versa 3, Fei, Hillsboro, United States) at an accelerating voltage of 5–10 kV. Prior to microscopic observation, the membranes were immersed in liquid nitrogen and then fractured to reveal their cross-section. The isoelectric point and zeta potential curves of the membranes were determined using an electrokinetic analyzer (SurPASS™ 3, Anton Paar, Graz, Austria). Contact angle measurements were performed using a goniometer (PG-1, Fibro System AB, Sweden) by employing the sessile drop method, where ten strips of dried membrane samples were inserted into the device. The porosity of each membrane was measured based on Equation 1, where ε (%) is the porosity, m_w (g) is the mass of the wet membrane, m_d (g) is the mass of dry membrane (treated at 40°C for 24 h), A (cm²) is the surface area of the membrane, T (cm) is the membrane thickness, and d (g/cm³) is the density of water density. Five samples of each membrane type were measured, and the average values were calculated.

$$\varepsilon = \frac{m_w - m_d}{A \cdot d \cdot T} \quad (1)$$

Micropollutants and WWTP effluent

Effluent from a local WWTP (Gliwice, Poland) was spiked with a sufficient volume of micropollutant (CAF, BZT, CBZ, BPA) stock solution (1 g/L in methanol) and used as the feed water in this study. Effluent samples were taken in July 2020 directly from the settling tank and stored in five-liter brown bottles in the refrigerator until processing (within seven days). The basic physical-chemical characteristics of these

effluents are presented in Table 2. The final concentration of each compound in the feed water was 1 mg/L. The physicochemical properties of the micropollutants are presented in Table 3.

Filtration tests

Ultrafiltration was carried out in cross-flow nanofiltration units (GE Osmonics) at a constant transmembrane pressure of 2.5 bar and a temperature of 22 ± 1°C. The system was equipped with a feed container (30 dm³) with a refrigerating system, rotameter, high-pressure pump, and manometer. The active surface area of the membrane was 144 cm². Before each experiment, the clean water flux was determined using ultrapure water. Each filtration run consisted of four cycles, including 60 min of filtration followed by forward flushing (FF) with deionized water for 30 s. The volume of the permeate was monitored to determine the permeability according to Equation 2:

$$L_p = \frac{V \cdot A^{-1} \cdot t^{-1}}{\Delta p} \quad (2)$$

where ($L \cdot m^{-2} \cdot h^{-1} \cdot bar^{-1}$; LMHB) is the permeability, V (L) is the permeate volume, A (m²) is the membrane surface area, t (h) is the permeate collection duration, Δp (bar) is the transmembrane pressure.

Membrane fouling evaluations

In this study, hydraulic resistances were measured to characterize the fouling behavior of the membranes used to treat WWTP effluent. The hydraulic resistances of the membranes and fouling layers were calculated using the resistance in a series model and Darcy's law based on the correlations in Equations 3–5.

$$k_{tot} = k_m + k_f \quad (3)$$

Table 2. Physical-chemical properties of WWTP effluent as taken

Parameter	Colour (mg Pt/L)	pH (-)	Absorbance (-) UV 254 nm	Phosphate phosphorus (mg P-PO ₄ /L)	Nitrate nitrogen (mg N-NO ₃ /L)	Phenolic index (mg/L)
Value	60	6.8	0.286	3.0	6.9	1.55

Table 3. Properties of micropollutants

Compound	CAF	BZT	CBZ	BPA
Molecular mass ¹ (g/mol)	194.2	119.1	236.3	228.3
Length ² (nm)	0.76	0.55	0.89	0.92
Width ² (nm)	0.59	0.1	0.65	0.6
Height ² (nm)	0.18	0.49	0.65	0.78
Eq. Width ³ (nm)	0.33	0.22	0.65	0.68
LogKow1 (-)	0.55	1.44	2.45	3.32
Solubility in water 20°C ¹ (mg/L)	21600	20000	17.7	<1
pKa ¹ (-)	10.4	8.2	13.9	10.1

¹ data taken from <https://pubchem.ncbi.nlm.nih.gov/>, ² measured with Avogadro software, ³ geometric mean of width and height

$$k_f = k_{irr} + k_{rev} \quad (4)$$

$$J = \frac{\Delta p}{\mu \cdot k} \quad (5)$$

where k (m^{-1}) is the hydraulic resistance (subscripts m , f , irr , rev , and tot correspond to the membrane, fouling, hydraulically irreversible fouling, hydraulically reversible fouling, and total fouling, respectively; J ($\text{m}^3 \cdot \text{m}^{-2} \cdot \text{s}^{-1}$) is the flux; Δp ($\text{kg} \cdot \text{s}^{-2} \cdot \text{m}^{-1}$) is the transmembrane pressure; μ ($\text{kg} \cdot \text{m}^{-1} \cdot \text{s}^{-1}$) is the dynamic viscosity of water at a given temperature. The membrane resistance (k_m) was measured using the clean membrane and ultrapure water prior to feed water filtration. The hydraulically irreversible fouling was determined from the flux after flushing, whereas the hydraulically reversible fouling was determined from the difference between the fouling and irreversible resistances.

Water quality analysis

The WWTP effluent treatment efficiency achieved by the ultrafiltration system was evaluated by monitoring typical quality parameters (e.g., color, phenolic index, absorbance, nitrate-nitrogen N-NO_4 , and phosphate-phosphorus P-PO_4) and the concentration of micropollutants. The phenolic index and the concentrations of N-NO_4 and P-PO_4 were determined spectrophotometrically with Merck test kits; the color and absorbance (UV 254 nm) were measured spectrophotometrically. The concentrations of micropollutants in the feed and permeate were measured with a 6500GC System GC-FID (YI Instrument Co. Ltd., Hoguey-dong, Anyang, Korea). The chromatograph was equipped with a $30 \text{ m} \times 0.25 \text{ mm}$ i.d. SLB® 5- μm fused silica capillary column with a $0.25 \mu\text{m}$ film thickness (Sigma Aldrich). Helium 5.0 was used as the carrier gas, and chromatographic separation of micropollutants was performed using a temperature program for the column oven for all substances ($80\text{--}320^\circ\text{C}$); the injector temperature was set at 240°C . Prior to analysis, the compounds were extracted from the samples via solid phase extraction (SPE; phase C18, Supelco), according to a previously developed method [Bohdziewicz et al. 2016].

The water quality was evaluated based on the micropollutant removal efficiency, which was calculated using Equation 6:

$$R = \frac{C_F - C_P}{C_F} * 100\% \quad (6)$$

where C_F and C_P (mg/L) represent the concentrations of pollutants in the feed water and permeate, respectively.

Additionally, during the ultrafiltration process, the adsorption of micropollutants onto the membranes was computed using Equation 7:

$$A = \left(1 - \frac{C_R V_R + C_P V_P}{C_F V_F}\right) \cdot 100\% \quad (7)$$

where A (%) is the degree of adsorption, C_r (mg/L) is the concentration of micropollutants in the retentate, and V_N , V_P , and V_R (L) are the volumes of the feed water, permeate, and retentate, respectively.

Results and discussion

Membrane characterization

Figure 1 shows the SEM micrographs of cross-sections of the pristine PES, PES-Hal, PES-SWCNT-COOH, and PES-TiO₂ membranes. All of the tested membranes exhibited a sponge-like structure with a dense top surface and a looser and more porous sublayer. Table 4 presents the porosity, contact angles, and thicknesses of these membranes, as well as the viscosity of the casting solutions. It is clear that the porosities of the nanocomposite mixed-matrix membranes were slightly lower than that of pristine PES. This can be explained by the higher viscosity of the casting solutions containing nanoparticles, which decrease the speed of phase inversion and, thus leading to lower porosity and higher thickness [Farjami et al. 2020]. The lower porosity of the PES-Hal, PES-SWCNT-COOH, and PES-TiO₂ membranes may be also a result of aggregated clusters of nanoparticles blocking internal pores [Vatantpour et al. 2021]. Mozia et al. reported that the porosity of a PES membrane modified by halloysite was lower than that of pristine PES [Mozia et al. 2019].

With the exception of PES-SWCNT-COOH, the nanocomposite membranes were thicker than pristine PES. The lower thickness of PES-SWCNT-COOH was attributed to the high water affinity of the carboxylic groups which enabled faster water penetration and solvent diffusion during phase inversion [Maximous et al. 2009].

Table 4 shows the effect of nanoparticles on membrane hydrophilicity. A significant increase in membrane hydrophilicity was observed for PES-SWCNT-COOH, which was ascribed to an effect of the carboxylic groups on the carbon nanotubes. The unexpected similarity between the hydrophilicity of PES-TiO₂ and PES-Hal with that of PES is likely related to the impact of membrane roughness on the contact angles. Due to nanoparticle agglomeration, the nanocomposite membranes show higher surface roughness, which results in higher contact angles [Mao et al. 2020].

Based on the zeta potential curves (Fig. 2), it is clear that the PES-Hal membrane exhibited much lower surface charge than the other prepared membranes. Moreover, an isoelectric point (IP) in the pH range of 2.4–8 was not observed for PES-Hal. The PES-SWCNT-COOH and PES-TiO₂ membranes had slightly lower IPs and charges compared with pristine PES. A stronger negative charge of a nanocomposite membrane is related to the oxygen-containing groups in its nanofiller [Kamińska et al. 2015, Mozia et al. 2019].

Figure 3 presents the clean water flux through the studied membranes at a transmembrane pressure (TMP) ranging from 2 to 5 bar. For all membranes, the water flux increased linearly as the TMP increased. These membranes exhibited different water permeability owing to the combined effects of various structural and surface properties, such as thickness, porosity, and hydrophilicity.

WWTP effluent treatment via ultrafiltration

The effect of the membranes on the treatment of WWTP effluent and removal of micropollutants is presented in Figures 4a and 4b. The membranes modified with nanoparticles achieved better treatment efficiency compared with pristine PES. According to Fig. 4a, the color was reduced by 72%, 70%,

and 65% following ultrafiltration with PES-SWCNT-COOH, PES-Hal, and PES-TiO₂, respectively. Lower reduction in color (59%) was noted for the PES membrane. The pristine PES also showed the lowest elimination degree of the absorbance at

UV-254 and the phenolic index. Color, phenolic index, and UV-254 absorbance are the quality parameters related to the content of organic pollutants in these samples. The pollutants could be retained in UF because of the sieve effect (high

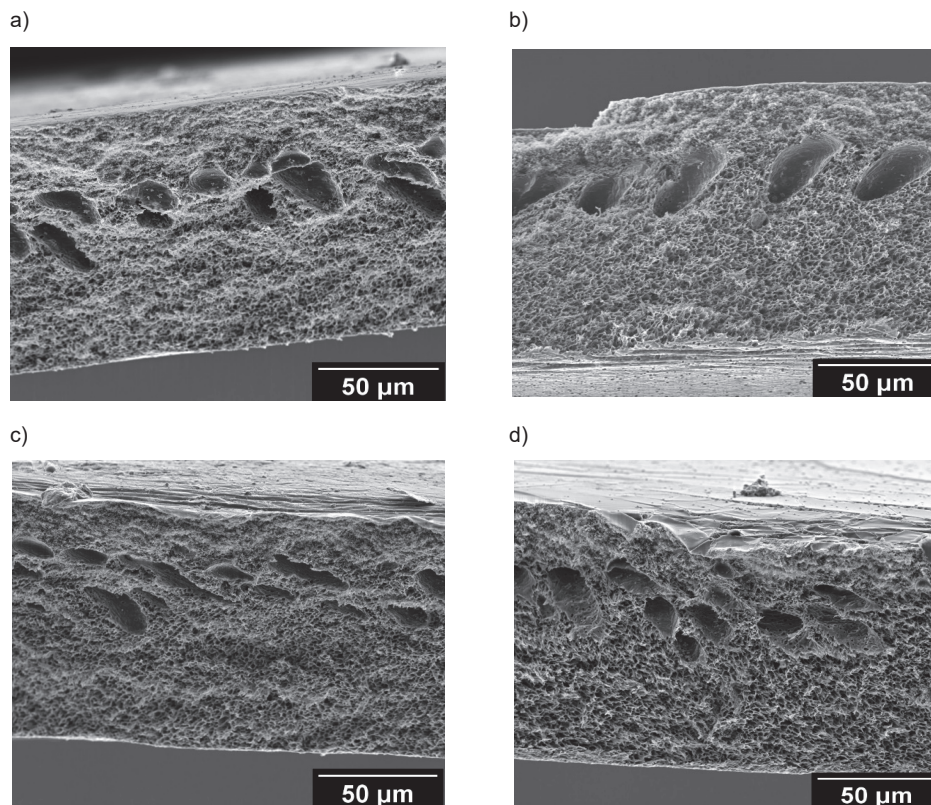


Fig. 1. SEM images of membrane cross-sections: (a) PES; (b) PES-Hal; (c) PES-SWCNT-COOH; (d) PES-TiO₂

Table 4. Properties of casting solution and membranes

Property	PES	PES-Hal	PES-SWCNT-COOH	PES-TiO ₂
Viscosity (mPa·s)	239	350	321	339
Porosity (%)	52±3.9	49±5.2	38±5.3	45±2.1
Membrane thickness (μm)	109.7±1.4	114.3±3.2	100.3±1.2	113.2±6.5
Contact angle of clean membrane (°)	72±4.1	76±4.5	77±3.5	65±3.3

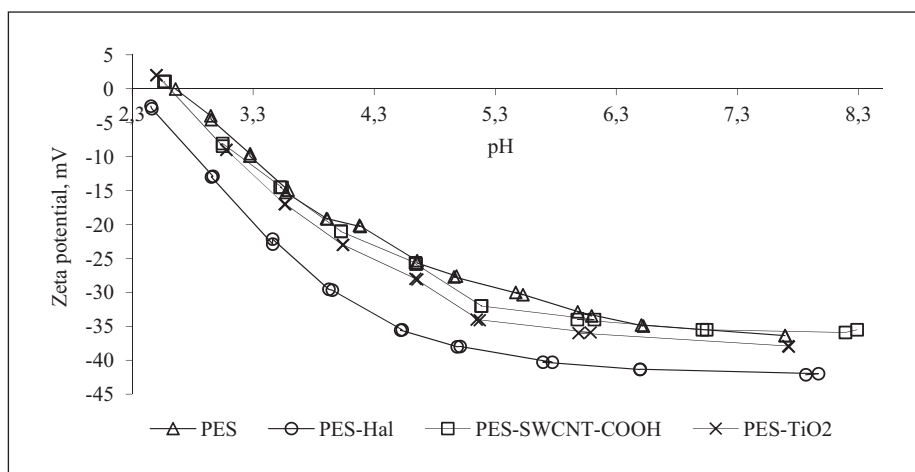


Fig. 2. Zeta potential curves of membranes

molecular weight organic compounds, such as proteins, polymers, and humic acids) or adsorption (low molecular weight organic compounds) [Hao et al. 2021]. Therefore, better removal of pollutants by the nanocomposite membranes was attributed to their lower porosity compared to pristine PES. Additionally, SWCNT-COOH and Hal are considered to be good sorbents [Gamoń et al. 2022, Marszałek 2022], thus, their presence in PES-Hal and PES-SWCNT-COOH membranes enhanced the separation of organic pollutants via adsorption [Buruga et al. 2019, Kamińska et al. 2015].

Nitrate nitrogen (N-NO_3^-) and phosphate phosphorus (P-PO_4^{3-}) removal were relatively low, i.e., from 8% to 45% and from 12% to 61%, respectively. Ultrafiltration is not a technique typically suitable for the removal of nutrients because of their ionic radii, which are smaller than the average pore size of the ultrafiltration membranes [Suhaimi et al. 2022]. A high retention of nutrients can be achieved through reverse osmosis, where changes in solubility and diffusivity comprise the dominant removal mechanism [Leo et al. 2011]. On the other hand, a slightly better reduction of nitrate nitrogen and phosphate phosphorus exhibited by PES-Hal compared with the other tested membranes could be attributed to the fact that halloysite contains aluminum oxides and silica. Aluminum oxides are active for the adsorption of anions, such as nitrate and phosphate [Saki et al. 2019]. Moreover, the PES-Hal membrane exhibited the lowest isoelectric point and zeta potential at $\text{pH} \sim 7$ (Fig. 2), which allowed ions to be rejected because of the enhanced repulsion forces between the ions and the membrane surface [Muthumareeswaran et al. 2014]. Interestingly, for all membranes, the retention of N-NO_3^- was lower than P-PO_4^{3-} retention. It can be explained by competition for adsorption active sites between nitrate nitrogen and phosphate phosphorus [Wang et al. 2021].

Figure 4b presents the retention of micropollutants for the nanocomposite membranes and pristine PES membrane. The performance of the membranes in terms of micropollutant removal decreased in the order: PES-SWCNT-COOH > PES-Hal > PES-TiO₂ \approx PES. The enhanced micropollutant removal by PES-SWCNT-COOH and PES-Hal was attributed to the adsorption of the micropollutants on carbon nanotubes and halloysite, respectively [Niedergall et al. 2014]. As shown in Fig. 5, the adsorption of micropollutants was the

highest for the PES-SWCNT-COOH membrane and then for PES-Hal.

The mechanism of organic micropollutant separation by a nanocomposite membrane can include the sieve effect, electrostatic forces, intermolecular interactions, and blocking or narrowing of pores by precipitated pollutant particles [Nguyen et al. 2021, Zhang et al. 2020]. The dominant mechanism among these potential options is determined by the physicochemical properties of the micropollutants, the nature of the feed, and the surface and structural properties of the membrane. The pK_a values for all micropollutants (Table 3) were higher than the pH of the feed, thus, the chemical form of these compounds was neutral. As a result, we can exclude the contribution of electrostatic repulsion in the separation of organic micropollutants. Interestingly, BPA and CBZ were removed to a greater extent than the less hydrophobic compounds with lower $\log K_{ow}$ values, i.e., CAF and BZT (Table 3). The higher the value of $\log K_{ow}$, the more hydrophobic the compound, and the higher its sorption affinity [Kamińska et al. 2018]. From Fig. 5, it is clear that the adsorption of micropollutants during ultrafiltration decreased in the order: BPA > CBZ > BZT > CAF. In other words, the hydrophilicity/hydrophobicity of compounds affected the degree of micropollutant removal because adsorption plays a crucial role in the separation of low molecular weight compounds during ultrafiltration [Nguyen et al. 2021, Zhang et al. 2020].

The retention of CAF by the PES, PES-Hal, and PES-TiO₂ membranes was not a result of adsorption (0%). In contrast, the retention of CAF by these membranes can be explained by the fact that preliminarily adsorbed pollutants from the feed clogged the pores, thereby narrowing the pores. In other words, membrane fouling and a probable cake layer enhanced the removal of micropollutants.

Membrane performance and fouling behavior

The hydraulic performance of membranes was evaluated based on permeability loss as a function of time. As shown in Fig. 6, the permeability decreased rapidly for the PES and PES-SWCNT-COOH membranes, whereas the permeability loss of PES-Hal and PES-TiO₂ within a single cycle was much lower. This distinction could be explained by different surface charges of these membranes. Owing to the stronger negative

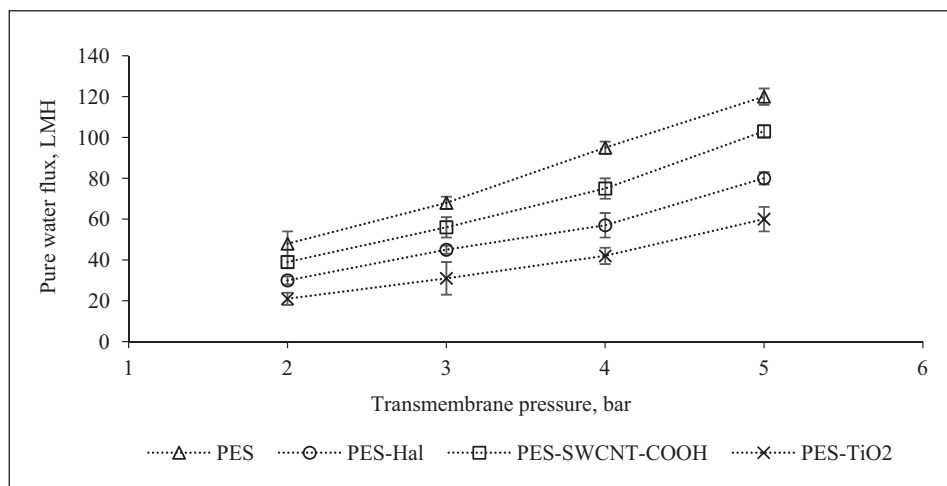


Fig. 3. Pure water flux as a function of transmembrane pressure for the tested membranes

surface charge of PES-TiO₂ and PES-Hal (Fig. 2), these membranes both exhibited excellent antifouling properties. Numerous researchers have proposed that the addition of nanofillers, such as halloysite or titanium dioxide, helps the membrane surface resist fouling [Arif et al. 2019, Mozia et al. 2019].

To further investigate this behavior, the reversible and irreversible resistances were calculated. As shown in Fig. 7,

a significant proportion of the increase in resistance for membranes modified with nanofillers was reversible, whereas it was irreversible for pristine PES. This result indicates that the deposition of pollutants on the surface of the PES membrane was relatively persistent, and a major part of the cake layer could not be removed by forward flushing (FF). In contrast, a higher contribution of reverse resistance for the nanocomposite membranes indicates much better removal

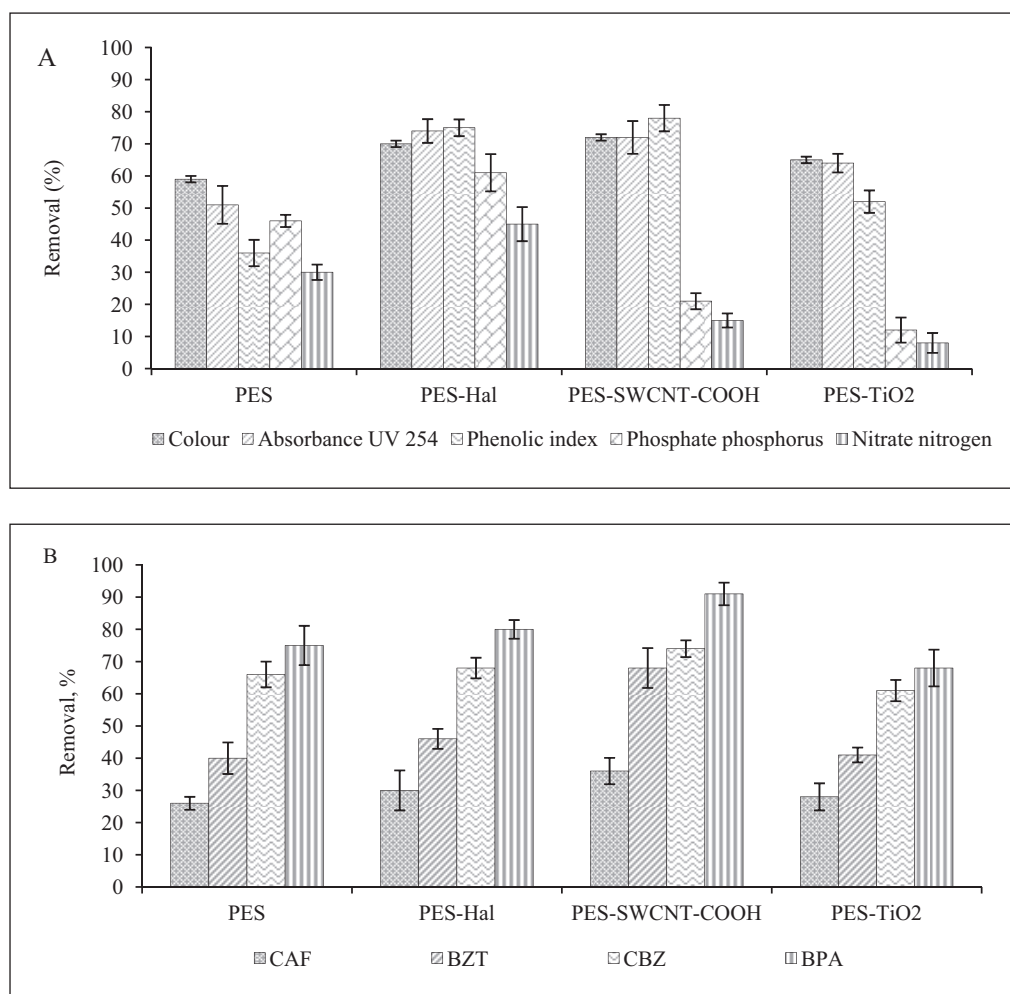


Fig. 4. Effect of membrane on WWTP effluent treatment (a) basic water quality parameters and (b) micropollutant removal

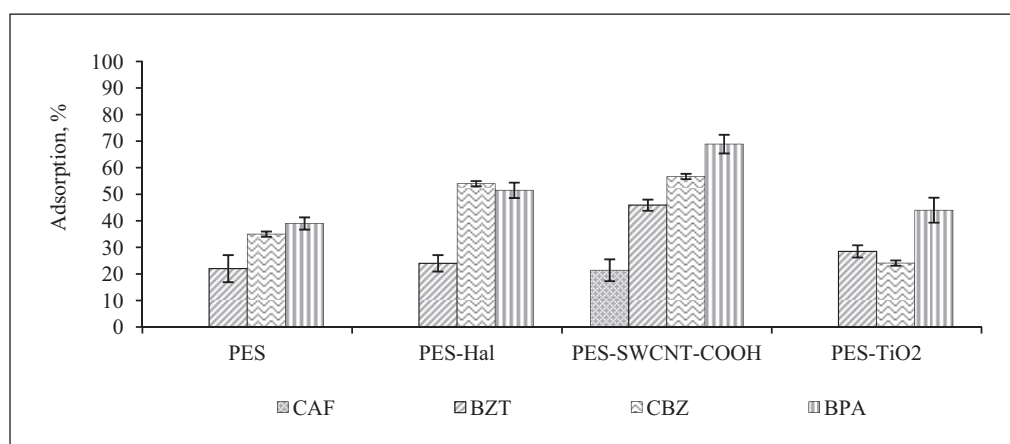


Fig. 5. Adsorption of micropollutants on membranes during ultrafiltration

of the cake layer by FF. These results can be explained by different physicochemical and structural properties of the membranes (e.g., porosity, contact angle, zeta potential, and roughness) [Inurria et al. 2019]. These properties influence the deposition of pollutants and the resulting permeability loss during filtration, as well as the removal of the cake layer by FF. It is well established that a more hydrophobic surface promotes the adsorption of pollutants. In other words, because of their higher contact angles (Table 4) and lesser degrees of negative surface charge (Fig. 2), the PES and PES-SWCNT-COOH membranes exhibited greater permeability loss (Fig. 6) than PES-Hal and PES-TiO₂. The lower adsorption/deposition of pollutants on the surface of the PES-TiO₂ membrane resulted in a thinner cake layer, which was likely easier to remove by FF [Kamińska et al. 2020]. The second factor influencing the formation of irreversible fouling is membrane porosity. Pollutants can penetrate and block the internal pores of more porous and open membranes. This explains why the pristine PES membrane showed the highest fouling irreversibility. In this case, even chemical cleaning or backflushing are not very effective [Adeniyi et al. 2020]. Another negative effect of the blocking of internal pores is manifested in the deterioration of the separation effect due to the accumulation of pollutants

inside the membranes and their passage through the membrane to the permeate.

Once the cake layer has been formed, its removal also depends on the membrane properties, in particular, the zeta potential and membrane roughness. A strong negative zeta potential weakens the adhesive force between the membrane surface and the pollutants forming the cake layer. This creates an electrostatic repulsion effect between the negatively-charged membrane and negatively-charged organic compounds, such as dissolved organic carbon (DOC) and natural organic matter (NOM), and other feed pollutants. We observed a rapid decrease in the permeability of the PES-SWCNT-COOH membrane during 60 min of filtration, but after FF, the membrane permeability returned to its initial value. This result indicated that the cake layer was removed following FF, and the membrane recovered its initial surface properties.

Conclusions

This study describes the treatment of WWTP effluent containing organic micropollutants through an ultrafiltration process with PES-based membranes modified with various types of nanofillers. The color, absorbance, phenolic index,

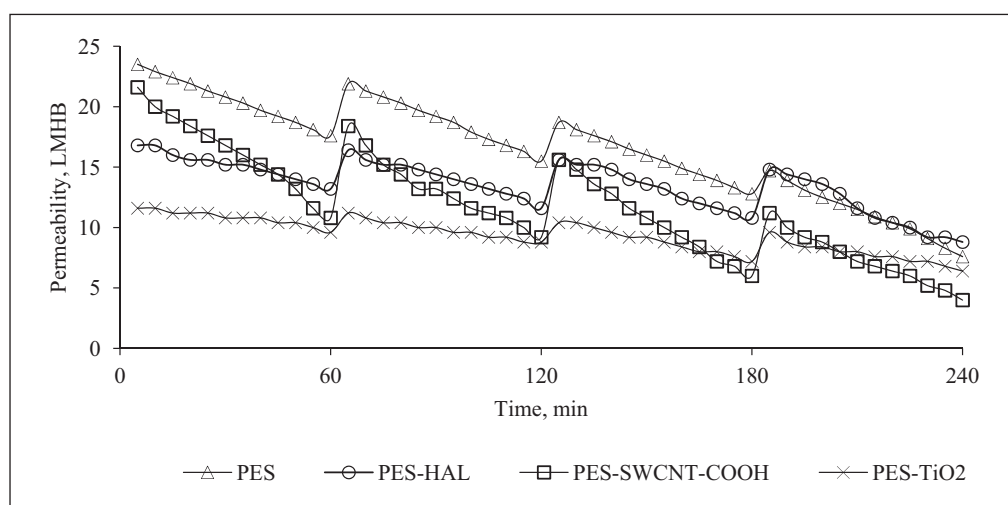


Fig. 6. Permeability loss as a function of ultrafiltration time for the prepared membranes

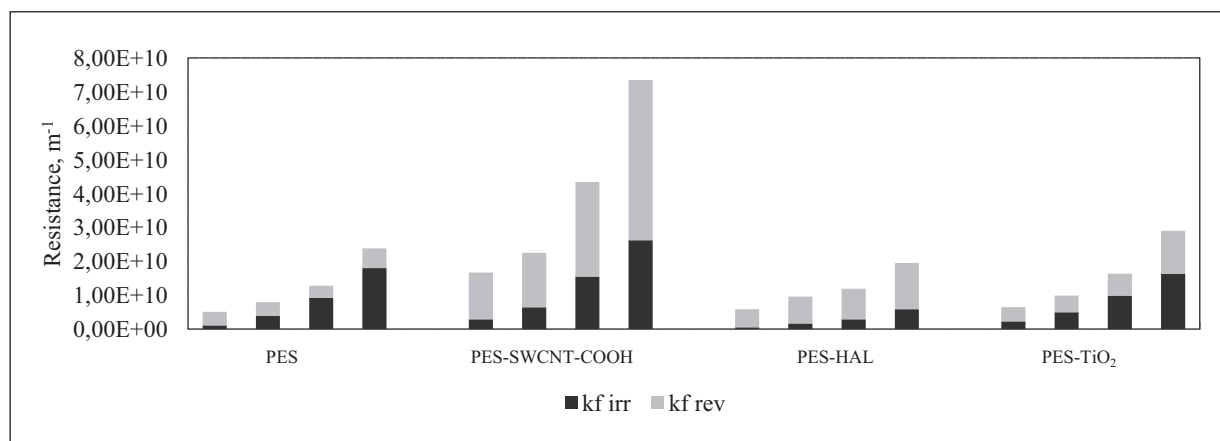


Fig. 7. Irreversible and reversible fouling resistances of ultrafiltration for all tested membranes. Each bar corresponds to the filtration cycles 1–4

and concentrations of phosphate phosphorus and nitrate nitrogen were reduced by up to 72%, 74%, 78%, 61%, and 45%, respectively. Ultrafiltration with the PES-Hal and PES-SWCNT-COOH membranes reduced the micropollutant concentration and improved the typical water quality parameters better than pristine PES. Among the evaluated nanocomposite membranes, the lowest removal performance was observed for PES-TiO₂. The halloysite and SWCNT-COOH, which were good sorbents on their own, enhanced the adsorption of pollutants on membranes, leading to superior removal efficiencies. Micropollutant removal varied greatly among the tested membranes owing to their distinct physicochemical properties. The removal of bisphenol A was the highest because of its high hydrophobicity.

Modified membranes improve antifouling properties, as evidenced by their increased fouling reversibility. In particular, PES-Hal achieved the highest treatment efficiency and showed the most effective antifouling properties. This was attributed to the enhanced adsorption/deposition of pollutants on the surface but at the same efficient removal of the deposited layer by FF.

References

- Adeniyi, A., Mbaya, R., Popoola, P., Gomotsegang, F., Ibrahim, I. & Onyango, M. (2020). Predicting the fouling tendency of thin film composite membranes using fractal analysis and membrane autopsy, *Alexandria Engineering Journal*, 59, 6, pp. 4397–4407, DOI: 10.1016/j.aej.2020.07.046
- Arif, Z., Sethy, N.K., Mishra, P.K. & Verma, B. (2019). Antifouling behaviour of PVDF/TiO₂ composite membrane: a quantitative and qualitative assessment, *Iranian Polymer Journal*, 19, 28, pp. 301–312, DOI: 10.1007/s13726-019-00700-y
- Bassyouni, M., Abdel-Aziz, M.H., Zoromba, M.Sh., Abdel-Hamid, S.M.S. & Drioli, E. (2019). A review of polymeric nanocomposite membranes for water purification, *Journal of Industrial and Engineering Chemistry*, 73, pp. 19–46, DOI: 10.1016/j.jiec.2019.01.045
- Bodzek, M., Konieczny, K. & Kwiecińska-Mydlak, A. (2021). New generation of semipermeable membranes with carbon nanotubes for water and wastewater treatment: Critical review, *Archives of Environmental Protection*, 47, 3, pp. 3–27, DOI: 10.24425/aep.2021.138460
- Bohdziewicz, J., Dudziak, M., Kamińska, G. & Kudlek, E. (2016). Chromatographic determination and toxicological potential evaluation of selected micropollutants in aquatic environment – analytical problems, *Desalination and Water Treatment*, 57, pp. 1361–1369, DOI: 10.1080/19443994.2015.1017325
- Bu, F., Gao, B., Yue, Q., Liu, C., Wang, W. & Shen, X. (2019). The Combination of Coagulation and Adsorption for Controlling Ultrafiltration Membrane Fouling in Water Treatment, *Water*, 11, pp. 1–13, DOI: 10.3390/w11010090
- Buruga, K., Song, H., Shan, J., Bolan, N., Thimmarajampet Kalathi, J. & Kim, K-H. (2019). A review on functional polymer-clay based nanocomposite membranes for treatment of water, *Journal of Hazardous Materials*, 379, pp. 1–27, DOI: 10.1016/j.jhazmat.2019.04.067
- Dudziak, M. & Burdzik-Niemiec, E. (2017). Ultrafiltration through modified membranes in wastewater treatment containing 17β-estradiol and bisphenol A, *Przemysł Chemiczny*, 96, pp. 448–452, DOI: 10.15199/62.2017.2.35. (in Polish)
- Esfahani, M.R., Aktij, S.A., Dabaghian, Z., Firouzjarei, M.D., Rahimpour, A., Eke, J., Escobar, I.C., Abolhassani, M., Greenlee, L.F., Esfahani, A.R., Sadmani, A. & Koutahzadeh, N. (2019). Nanocomposite membranes for water separation and purification: Fabrication, modification, and applications, *Separation and Purification Technology*, 213, pp. 465–499, DOI: 10.1016/j.seppur.2018.12.050
- Farjami, M., Vatanpour, V. & Moghadassi, A. (2020). Effect of nanobiochmite/poly(ethylene glycol) on the performance and physiochemical attributes EPVC nano-composite membranes in protein separation, *Chemical Engineering Research and Design*, 156, pp. 371–383, DOI: 10.1016/j.cherd.2020.02.009
- Gamoń, F., Tomaszewski, M., Cema, G. & Ziemińska-Buczyńska, A. (2022). Adsorption of oxytetracycline and ciprofloxacin on carbon-based nanomaterials as affected by pH, *Archives of Environmental Protection*, 48, 2, pp. 34–41, DOI: 10.24425/aep.2022.140764
- Ghaemi, N., Madaeni, S.S., Alizadeh, A., Rajabi, H. & Daraei, P. (2011). Preparation, characterization and performance of polyethersulfone/organically modified montmorillonite nanocomposite membranes in removal of pesticides, *Journal of Membrane Science*, 382, pp. 135–147, DOI: 10.1016/j.memsci.2011.08.004
- Haas, R., Opitz, R. & Grischek, T. (2019). The AquaNES Project: Coupling Riverbank Filtration and Ultrafiltration in Drinking Water Treatment, *Water*, 11, pp. 1–14, DOI: 10.3390/w11010018
- Hao, S., Jia, Z., Wen, J., Li, S., Peng, W., Huang, R. & Xu, X. (2021). Progress in adsorptive membranes for separation – A review, *Separation and Purification Technology*, 255, 117772, DOI: 10.1016/j.seppur.2020.117772
- Inurria, A., Cay-Durgun, P., Rice, D., Zhang, H., Seo, D.-K., Lind, M.L. & Perreault, F. (2019). Polyamide thin-film nanocomposite membranes with graphene oxide nanosheets: Balancing membrane performance and fouling propensity, *Desalination*, 451, pp. 139–147, DOI: 10.1016/j.desal.2018.07.004
- Kamińska, G. (2022). Modification of ultrafiltration membranes with nanoparticles and their application, Wydawnictwo Politechniki Śląskiej, Gliwice 2022. (in Polish)
- Kamińska, G. & Bohdziewicz, J. (2018). Separation of selected organic micropollutants on ultrafiltration membrane modified with carbon nanotubes. *Ochrona Środowiska*, 40, 4, pp. 37–42. (in Polish)
- Kamińska, G., Bohdziewicz, J., Calvo, J.I., Prádanos, P., Palacio, L. & Hernández, A. (2015). Fabrication and characterization of polyethersulfone nanocomposite membranes for the removal of endocrine disrupting micropollutants from wastewater. Mechanisms and performance, *Journal of Membrane Science*, 493, pp. 66–79, DOI: 10.1016/j.memsci.2015.05.047
- Kamińska, G., Bohdziewicz, J., Palacio, L., Hernández, A. & Prádanos, P. (2016). Polyacrylonitrile membranes modified with carbon nanotubes: characterization and micropollutants removal analysis, *Desalination and Water Treatment*, 57, pp. 1344–1353, DOI: 10.1080/19443994.2014.1002277
- Kamińska, G., Pronk, W. & Traber, J. (2020). Effect of coagulant dose and backflush pressure on NOM membrane fouling in inline coagulation-ultrafiltration, *Desalination and Water Treatment*, 199, pp. 188–197, DOI: 10.5004/dwt.2020.25657
- Leo, C.P., Chai, W.K., Mohammad, A.W., Qi, Y., Hoedley, A.F.A. & Chai, S.P. (2011). Phosphorus removal using nanofiltration membranes, *Water Science and Technology* 64, pp. 199–205, DOI: 10.2166/wst.2011.598
- Mao, Y., Huang, Q. Meng, B., Zhou, K., Liu, G., Gigliuzza, A., Drioli, E. & Jin, W. (2020). Roughness-enhanced hydrophobic graphene oxide membrane for water desalination via membrane distillation, *Journal of Membrane Science*, 611, 118364, DOI: 10.1016/j.memsci.2020.118364
- Marszałek, A. (2022). Encapsulation of halloysite with sodium alginate and application in the adsorption of copper from

- rainwater, *Archives of Environmental Protection*, 48, 1, pp. 75–82, DOI: 10.24425/aep.2022.140546
- Maximous, N., Nakhla, G., Wan, W. & Wong, K. (2009). Preparation, characterization and performance of Al₂O₃/PES membrane for wastewater filtration, *Journal of Membrane Science*, 341, pp. 67–75, DOI: 10.1016/j.memsci.2009.05.040
- Mozia, S.; Grylewicz, A.; Zgrzebnicki, M.; Darowna, D. & Czyżewski, A. (2019). Investigations on the properties and performance of mixed matrix polyethersulfone membranes modified with halloysite nanotubes, *Polymers-Basel*. 11, 671, pp. 1–18, DOI: 10.3390/polym11040671
- Muthumareeswaran, M.R. & Agarwal, G.P. (2014). Feed concentration and pH effect on arsenate and phosphate rejection via polyacrylonitrile ultrafiltration membrane, *Journal of Membrane Science*, 468, pp. 11–19, DOI: 10.1016/j.memsci.2014.05.040
- Nasir, A., Masood, F., Yasin, T. & Hamed, A. (2019). Progress in polymeric nanocomposite membranes for wastewater treatment: Preparation, properties and applications, *Journal of Industrial and Engineering Chemistry*, 79, pp. 29–40, DOI: 10.1016/j.jiec.2019.06.052
- Nguyen, M.N., Trinh, P.B., Butkhardt, C.J. & Schafer, A.I. (2021). Incorporation of single-walled carbon nanotubes in ultrafiltration support structure for the removal of steroid hormone micropollutants, *Separation and Purification Technology*, 264, 118405, DOI: 10.1016/j.seppur.2021.118405
- Niedergall, K., Bach, M., Hirth, T., Tovar, G.E.M. & Schiestel, T. (2014). Removal of micropollutants from water by nanocomposite membrane adsorbers, *Separation and Purification Technology*, 131, 27, pp. 60–68, DOI: 10.1016/j.seppur.2014.04.032
- Rogowska, J., Cieszyńska-Semenowicz, M., Ratajczyk, W. & Wolska, L. (2020). Micropollutants in treated wastewater, *Ambio*, 49(2), pp. 487–503, DOI: 10.1007/s13280-019-01219-5
- Saki, H., Alemayehu, E., Schomburg, J. & Lennartz, B. (2019). Halloysite nanotubes as adsorptive material for phosphate removal from aqueous solution, *Water* 11, 2, 203, DOI: 10.3390/w11020203
- Shaban, M., AbdAllah, H., Said, L. & Ahmed, A.M. (2019). Water desalination and dyes separation from industrial wastewater by PES/TiO₂NTs mixed matrix membranes, *Journal of Polymer Research*, 26, 181, pp. 1–12, DOI: 10.1007/s10965-019-1831-4
- Shakak, M., Rezaee, R., Maleki, A., Jafari, A., Safari, M., Shahmoradi, B., Daraei, H. & Lee, S.-M. (2019). Synthesis and characterization of nanocomposite ultrafiltration membrane (PSF/PVP/SiO₂) and performance evaluation for the removal of amoxicillin from aqueous solutions, *Environmental Technology & Innovation*, 17, 100529, DOI: 10.1016/j.eti.2019.100529
- Suhalim, N.S., Kasim, N., Mahmoudi, E., Shamsudin, I.J., Mohammad, A.W., Zuki, F.M. & Jamari, N. (2022). Rejection Mechanism of Ionic Solute Removal by Nanofiltration Membranes: An Overview, *Nanomaterials*, 12, 437, DOI: 10.3390/nano12030437
- Vatanpour, V., Mansourpanah, Y., Soroush Mousavi Khadem, S., Zinadini, S., Dizge, N., Reza Ganjali, M., Mirsadeghi, S., Rezapour, M., Reza Saeb, M. & Karimi-Male, H. (2021). Nanostructured polyethersulfone nanocomposite membranes for dual protein and dye separation: Lower antifouling with lanthanum (III) vanadate nanosheets as a novel nanofiller, *Polymer Testing*, 94, pp. 107040, DOI: 10.1016/j.polymertesting.2020.107040
- Vatanpour, V., Madaeni, S.S., Rajabi, L., Zinadini, S. & Derakhshan, A.A. (2012). Boehmite nanoparticles as a new nanofiller for preparation of antifouling mixed matrix membranes, *Journal of Membrane Science*, 401–402, pp. 132–143, DOI: 10.1016/j.memsci.2012.01.040
- Wang, S., Yao, S., Du, K., Yuan, R., Chen, H., Wang, F. & Zhou, B. (2021). The mechanisms of conventional pollutants adsorption by modified granular steel slag, *Environmental Engineering Research*, 26, 1, 190352, DOI: 10.4491/eer.2019.352
- Zhang, J., Nguyen, M.N., Li, Y., Yang, C. & Schafer, A.I. (2020). Steroid hormone micropollutant removal from water with activated carbon fiber-ultrafiltration composite membranes, *Journal of Hazardous Materials*, 391, 122020, DOI: 10.1016/j.jhazmat.2020.122020
- Zhang, X., Wang, D.K., Lopez, D.R.S. & Diniz da Costa, J. (2014). Fabrication of nanostructured TiO₂ hollow fiber photocatalytic membrane and application for wastewater treatment, *Chemical Engineering Journal*, 236, pp. 314–322, DOI: 10.1016/j.cej.2013.09.059

Porównanie efektywności i foulingu ultrafiltracyjnych membran nanokompozytowych – zmieszana matryca podczas ultrafiltracji odpływów z oczyszczalni ścieków

Streszczenie: Celem pracy było porównanie zdolności separacyjnych i tendencji do foulingu trzech membran nanokompozytowych podczas oczyszczania odpływu z oczyszczalni, który domieszkowano mikrozanieczyszczeniami organicznymi. Membrany nanokompozytowe typu mieszana matryca preparowano metodą inwersji. Membrany nanokompozytowe domieszkowano halozytem, nanotlenkiem ditytanu lub jednościenne nanorurkami węglowymi funkcjonalizowanymi grupami karboksylowymi (SWCNT-COOH). Membrany nanokompozytowe charakteryzowały się niższą porowatością i silniejszym ujemnym ładunkiem powierzchniowym dzięki dodaniu hydrofilowych nanowypełniaczy. Membrana PES-Hal została uznana za najbardziej korzystną pod względem wydajności hydraulicznej i współczynników retencji mikrozanieczyszczeń. Było to wynikiem zwiększonej adsorpcji zanieczyszczeń na powierzchni membrany i tworzeniu łatwo usuwalnej warstwy placka (tj. oporu wywołanego foulingiem odwracalnym). Membrana PES-SWCNT-COOH charakteryzowała najwyższymi współczynnikami retencji, ale również dużą utratą przepuszczalności. Natomiast PES-TiO₂ wykazywała doskonałe właściwości przeciwpowrostowe, ale słabsze właściwości separacyjne względem badanych mikrozanieczyszczeń.